NUMERICAL SIMULATION OF HEAT AND MASS TRANSFER, MIXTURE FORMATION IN COMBUSTION CHAMBER OF GAS TURBINE ENGINE

A.A. SVIRIDENKOV, P.D. TOKTALIEV AND V.V. TRETYAKOV

Baranov Central Institute of Aviation Motors (CIAM)
Moscow, Russia
e-mail: toktalievp@ciam.ru

Summary. Results of numerical simulation of mixture formation and liquid fuel evaporation processes in combustion chamber of gas turbine engine are presented. Simple mathematical model of non-equilibrium evaporation of liquid fuel is proposed, model postulates dependence of droplet evaporation rate from fuel vapor partial pressure above the droplet surface. To estimate significance of proposed dependence numerical simulation of isothermal and non-isothermal turbulent flow in computational domain, which imitates geometry of combustion chamber, is performed. For isothermal case influence of interfacial impulse exchange, related with discrete phase propagation, on flow structure is estimated. In non-isothermal case it was shown, that taking into account non-equilibrium of evaporation in proposed way is essential at temperatures of gas phase T<600...800 K.

1 INTRODUCTION

Aircraft engine performance depends strongly of the efficiency of mixing and burning of the liquid fuel in the combustion chamber. Description of propagation and evaporation of the discrete liquid or solid phase of the fuel in challenging conditions occurring in the combustion chambers is actual problem for the modern aircraft engines. This problem is directly related to the task of describing the turbulent multi-component flow (i.e. bulk phase) in the combustion chamber. Goal of this paper is to develop a numerical method for coupled solution of the problems of computational fluid dynamics, the propagation and evaporation of the drop-liquid phase of fuel in the non-equilibrium regime in the combustion chamber of an aircraft engine.

First attempts of description of heating and evaporation of the drop phase of fuel for the following ignition have been made in end of the 19th century. This activity has been intended for development of the internal combustion engines for the liquid fuels. So in 1877 one of the first models of evaporation of a single drop has been proposed, this model uses an assumption that the evaporation process depends only on the diffusion of vapors from the surface [1]. In the first half of the 20th century mathematical description of the heating and evaporation of the fuel droplets has been developed, however, most models used in practice were based on experimental data and decoupled description of the drop-liquid phase and surrounding gas. These models are presented in the survey papers [1, 2] and the references therein. Development of computational fluid dynamics (CFD) in the second half of the 20th century not only allowed us to consider the problem of the drop-liquid phase and the surrounding gas flow in coupled formulation, but also raised the task of the computational complexity of the discrete phase models. This period until the mid-90s is characterized by the use of methods of continuum mechanics and the refinement of the mechanisms and characteristics of mass,

momentum, energy transfer in the liquid-liquid phase and the surrounding gas. Continuous medium mechanics and more accurate definition of the mechanisms and characteristics of mass, momentum, energy transfer in the droplet-liquid phase and the surrounding gas have been used until the mid-90s. Mathematical models of heating and evaporation of the drop-liquid phase and their application are given in [3-8]. In the last 20-30 years the multi-component structures of the discrete phase and the evaporation kinetics have been used for description of the heating and evaporation of the drop-liquid phase. Extended survey of these models can be found in the monograph [9] and [10-12]. A number of particular problems such as evolution of droplet shape, computation of real properties of the bulk and discrete phases and features of coalescence and decay of individual drops are discussed in [13-15]. Analytical solutions in the form of Stokes and Oseen for individual drops are often used at low Reynolds numbers (Re <100) [16].

Now all the mathematical models for the heating and evaporation of the discrete drop-liquid phase in a turbulent flow can be divided into several groups [15] in order of increasing complexity and the computational efforts required: equilibrium models of stationary heat transfer of the drop with the surrounding medium (this case corresponds to the same droplet temperature in time and over the entire volume of the droplet), models using the approximation of the infinite molecular thermal conductivity of the droplet liquid, models with finite heat conductivity taking into account the flow inside the drop and model based on the solution of the full Navier-Stokes equations for two-phase flow. Application of models of the last group for solving engineering problems needs impressive computational efforts; therefore, results of such computation are used for the verification of models of the first groups. In addition, the most engineering applications assume that the sizes of individual droplets (d) are small in comparison with the characteristic linear dimensions of the flow L (i.e. $d \ll L$), so the dimensions of the droplets are neglected. Thus, the problem of coupled computation of the discrete phase and the flow field reduces to solving the Navier-Stokes equations for the bulk phase and the trajectory problem for a set of material drop-points. Local heat and mass transfer problem can be solved separately for each of drop-point.

The models can be classified by the criterion of equilibrium of the single drop evaporation. In the equilibrium approximation it is assumed that the vapor near the interface is saturated and the evaporation rate of the liquid from the surface of the drop does not depend on the vapor concentration near its surface. This approximation is valid for large heat fluxes to a drop [17] and with enough accuracy corresponds to the typical conditions in the combustion chamber with the initial temperature of the discrete phase $T_f \sim 300$ K and the temperatures of the bulk flux $T > 1000$ K. However, heat fluxes into the drop can be significantly less on the transitional modes of the combustion chamber or in the preheating of the fuel-air mixture.

Goal of this paper is formulation of the mathematical model of the heating and non-equilibrium evaporation of the drop-liquid phase of the fuel for real conditions of the combustion chamber of the gas turbine engine and also determination of the temperature range of the bulk phase with account of non-equilibrium effects. Also the paper presents the results of mathematical modeling of the complex physicochemical process of heating and evaporation of the discrete phase of fuel in the combustion chamber of an aircraft engine using the proposed mathematical model.

2   MODEL OF DROP-LIQUID FUEL EVAPORATION

Coupled solution of the problem of flow field and individual droplet characteristics determination can be build by sequential determination of droplet parameters and then using this data in solution procedure of Navier-Stokes equations for bulk phase. In this approach, the exchange of mass, momentum and energy between the bulk and discrete phases is described by source terms in Navier-Stokes equations and heat-and-mass transfer of the drop equations. Usually these source terms are calculated locally for each node (volume) of computational domain in case of using mesh methods for numerical solution. Thus, it is possible to use various numerical algorithms to solve aerodynamic, trajectory problems, the problem of heat-and-mass transfer of a drop. Matching of the problems can be accomplished by exchanging for each cell in computational domain the values of the change in the mass of liquid and vapor, momentum, and energy.

The calculation of the flow field in this paper is based on the solution of the unsteady Navier-Stokes equations in the framework of the detached vortex method [18]. For the subgrid viscosity, the Smagorinsky model with the constant $C=0.1$ is used. The computational procedure is based on the SIMPLEC algorithm [19]. The solution of the trajectory problem is carried out by the method of [20] and is based on the solution of a system of ordinary differential equations with initial conditions describing the motion of droplets, each of equations has the following form:

$$m_i(t)\ddot{X}_i = F_{r,i}(t, X_i, \dot{X}_i), i = 1..N$$

$$t = 0 : X = X_{i,0}, \dot{X} = \dot{X}_{i,0}$$

here i - number of droplet, $m_i(t)$ - mass of i-th droplet, X - vector of droplet coordinates, $F_{r,i}$ - resistance force acting on the droplet when it moves. The modeling of the droplets heating and evaporation processes in this paper is based on integral approach [4]. Thus, the iterative process of heat and mass transfer calculation for each time step can be organized according to the following scheme:

1. Set the initial values of all variables - pressure p, velocity V, temperature T, mass fractions of vapor and air Y_i for bulk phase, coordinates and velocities for all droplets $X_i, \dot{X}_i$, diameters and surface temperatures for all droplets $d_i, T_{p,i}$;

2. Solution of gas-dynamic problem (Navier-Stokes equations), ODE system for droplet motion, equations of heat and mass transfer for each of the droplets;

3. Updating the source terms in the Navier-Stokes equations associated with the interphase exchange of mass, momentum and energy;

4. Checking the convergence, advancement to the next time step.

Let us consider more closely the problem of determining the characteristics of a single droplet for known local values of bulk phase characteristics at the time $t=t_i$. From the balance of heat fluxes on the surface of droplet of radius r_d, the following transcendental equation can be obtained for determining the rate of evaporation of a droplet [4]:

$$\frac{dm}{dt} = -\frac{4\pi \cdot r_d \lambda}{C_p} \ln\left[1 + \frac{C_p(T - T_d)}{L_V + \dfrac{Q_H}{dm/dt}}\right]. \tag{1}$$

Here m – mass of the droplet, T_d – droplet surface temperature, T – temperature of bulk phase in computational cell with the droplet, C_p – bulk phase specific heat coefficient under constant pressure, λ – bulk phase heat conduction coefficient, L_V – latent heat of evaporation, Q_H – heat flux to droplet, leading to droplet heating without evaporation:

$$Q_H = 4\pi \cdot r_d \alpha (T - T_d),$$ (2)

where α - heat transfer coefficient between droplet and surrounding bulk phase. As $\dfrac{dm}{dt} = \dfrac{d}{dt}\left(\dfrac{\pi d_d^3 \rho_d}{6}\right) = \dfrac{\pi d_d^2 \rho_d}{2}\dfrac{d}{dt}(d_d)$, where d_d – droplet diameter, ρ_d – liquid of the droplet mass density, then equation (1) takes the following form:

$$\frac{d}{dt}d_d = -\frac{4\lambda}{\rho_d C_p d_d}\ln\left[1 + \frac{C_p(T - T_d)}{L_V + \dfrac{Q_H}{dm/dt}}\right].$$ (3)

In case of equilibrium evaporation, when $Q_H = 0$, equations (1) and (3) are transformed into

$$\frac{dm}{dt} = -\frac{4\pi \cdot r_d \lambda}{C_p}\ln\left[1 + \frac{C_p(T - T_d)}{L_V}\right],$$

$$\frac{d}{dt}d_d = -\frac{4\lambda}{\rho_d C_p d_d}\ln\left[1 + \frac{C_p(T - T_d)}{L_V}\right].$$

Equating the mass fluxes through a spherical surface of radius r and the surface of a droplet of radius r_d and assuming that the droplet evaporation rate is determined by the diffusion of vapors from its surface, one can obtain the following equation, which relates the droplet evaporation rate with the distribution of fuel vapor concentrations, see, for example [4] and [10]:

$$\frac{dm}{dt} = \frac{4\pi \cdot r^2 D_V \rho}{1 - Y}\frac{dY}{dr},$$ (4)

where Y – dimensionless vapor concentration, ρ – density of gas mixture (air and vapor), D_V – vapor diffusion coefficient. Integration of this equation under the assumption that the values of ρ and D_V can be replaced by their mean values gives the following expression for the distribution of the dimensionless vapor concentration Y over the radius r:

$$\frac{1 - Y}{1 - Y_\infty} = \left(\frac{1 - Y_d}{1 - Y_\infty}\right)^{r_d/r},$$

where Y_d and Y_∞ – dimensionless vapor concentration at the droplet surface and in the surrounding space respectively.

It can be noted, that in equation (1) function under the logarithm sign has a maximum value at $Q_H = 0$, as in the equilibrium evaporation case. For normal liquids, for example water

and kerosene, $C_p \approx 10^3$ J/K, $L_V \approx 5 \cdot 10^5$ J/kg. Then, at low gas flow tempearatures of the order 600 K and initial droplets temperatures of the order of 300 K, $\Delta T \approx 300$ K and $x = C_p \Delta T / L_V \approx 0.6$, that is, less than 1. In this case, equation (1) can be represented in the form: $\dfrac{dm}{dt} = -\dfrac{4\pi \cdot r_d \lambda}{L_V + \dfrac{Q_H}{dm/dt}} (T - T_d)$ or

$$\frac{dm}{dt} = \left[1 + \frac{4\pi \cdot r_d \lambda (T - T_d)}{L_V \dfrac{dm}{dt} + Q_H} \right]^{-1}. \tag{5}$$

Equation (5) allows to find the rate of droplets evaporation at low temperatures of the gas flow (bulk phase). Let's find the rate of heating of a single droplet assuming that its heating takes place so fast that the temperature of the droplet surface is approximately equal to the temperature of the liquid inside the droplet.

The heat flux into the droplet Q is equal to the sum of heat fluxes associated with the heating of droplet Q_H, droplet evaporation Q_V and the loss of heat, related with vapors convection (neglecting radiation heat flux). The equations of heat balance on the surface of a droplet of radius r_d and on the sphere of radius r have the following form:

$$Q = C_d m \frac{dT_d}{dt} + L_V \frac{dm}{dt} - C_{p,V} T_d \frac{dm}{dt}$$

$$Q = 4\pi r^2 \lambda \frac{dT}{dr} - C_p T_d \frac{dm}{dt}.$$

In the last equation, the first term on the right-hand side represents the heat flux to the droplet due to the thermal conductivity of the gas: $Q_H = 4\pi r^2 \lambda \dfrac{dT}{dr}$, and the second represents the convective heat losses associated with vapor motion.; C_d − specific heat of a droplet liquid, $C_{p,V}$− vapor specific heat coefficient at constant pressure. Equating the heat fluxes through the spherical surfaces of the droplet and in the surrounding space and integrating this equation over the radius from r_d to ∞ and from T_d to T in temperatures, assuming that the values of the quantities in the equation can be replaced by their mean values, one can obtain:

$$\frac{dT_d}{dt} = \frac{1}{mC_d} \left[4\pi \cdot r_d \lambda (T - T_d) - \frac{dm}{dt} (L_V - C_p T + C_{p,V} T_d) \right].$$

This equation describes the heating of the droplet and differs from the analogous equation of [21], where it is assumed that $C_{p,V} T_d = C_p T$ and where the heat Q_H is calculated using the heat transfer coefficient of the droplet with the surrounding medium α, see (2). The corresponding equation of [4] is written for the case $dm/dt = 0$.

To obtain the dependence of the droplet heating rate on the distribution of the vapor concentration in the space surrounding the droplet, it is necessary to solve together the heat transfer and droplet evaporation equations, which have the following form [4]:

$$4\pi \cdot r^2 \lambda_m \frac{dT}{dr} = \frac{dm}{dt}(L_V + C_{p,m}T - C_{p,V}T_d) + Q_H,$$

$$\frac{dm}{dt} = 4\pi \cdot r^2 D_V \rho_m \frac{dY_V}{dr} + Y_V \frac{dm}{dt}.$$

In the latter expression, the first term on the right-hand side is the vapor mass flux due to diffusion, the second is the vapor mass flux due to convection (the quantities associated to the mixture are denoted by the subscript "m"). Eliminating the radial coordinate from the system of equations, one can obtain after transformations:

$$\frac{dT}{\kappa(T-\alpha)} = \frac{dY_V}{1-Y_V},\tag{6}$$

where $\kappa = \dfrac{D_V \rho_m C_{p,m}}{\lambda_m}$, $\alpha = \dfrac{L_V}{C_{p,m}} - \dfrac{C_{p,V}T_d}{C_{p,m}} + \dfrac{Q_H}{dm/dt \, C_{p,m}}$. Integration of (6) with respect to T from T_d to T and from Y to Y_∞ to $Y_{V,d}$ assuming that κ and α are independent from the radial coordinate gives $\alpha(1-\zeta) = T_d \, \zeta - T$, where $\varsigma = \left(\dfrac{1-Y_{V,d}}{1-Y_\infty}\right)^\kappa$. Since $Q_H = C_d m \dfrac{dT_d}{dt}$, then after transformations:

$$\frac{dT_d}{dt} = \frac{1}{m}\frac{dm}{dt}\left[\frac{C_{p,V}T_d}{C_d} - \frac{L_V}{C_d} + \frac{C_{p,m}(T_d\varsigma - T)}{C_d(1-\varsigma)}\right].\tag{7}$$

Equation (7) expresses dependence of the droplet heating rate on its evaporation rate, on its temperature and ambient temperature, on the distribution of the vapor concentration, and on the properties of the air-vapor mixture and droplet liquid. Note that integrating the equation (4) in the ranges (r_d, r_∞) and (Y_d, Y_∞) assuming that the values of ρ and D_V can be replaced by their mean values, gives the following expression for the droplet evaporation rate, which can be used for solving equation (7):

$$\frac{dm}{dt} = -4\pi D_V \rho_m r_d L_V (1+B_m),\tag{8}$$

where B_m - mass transfer coefficient: $B_m = \left(\dfrac{Y_\infty - Y_d}{1-Y_\infty}\right)$.

According to [22] mass fractions of fuel vapor near the droplet surface Y_d can be expressed in the following way:

$$Y_d = \frac{1}{\left[1+\left(\dfrac{p}{p_v}-1\right)\dfrac{\mu_g}{\mu_l}\right]},$$

where p – pressure in the surrounding medium, p_v – saturation vapor pressure near the droplet surface, μ_g - molecular weight of air-vapor mixture in the droplet surrounding medium, μ_l -

molecular weight of droplet liquid. To calculate saturation vapor pressure, Van der Waals equation can be used [22]:

$$p_v = \exp(A - B/(T_d - 43)),$$

here A and B − Van der Waals constants, T_d - droplet surface temperature. Note that if the saturating vapor pressure near the droplet surface, p_v, is equal to the gas pressure in the surrounding medium, p , then $T_d = T_{vap}$, where T_{vap} - evaporation temperature of the droplet:

$$T_{vap} = 43 + \frac{B}{A - \ln p}.$$

The heating of the droplet occurs as long as the temperature of the droplet is less than its equilibrium value, T_e, such that all the heat absorbed by the droplet goes to its evaporation and is tranferred to the fuel vapor. This situation corresponds to the zero value of Q_H in formulas (1), (3), (6) and expression in square brackets in (5). The coupled solution of the heat balance equation (5) and the mass transfer equation (8) gives in this case following expression, see, for example, [4]:

$$T_e = T - L_V \frac{\zeta - 1}{C_{p,m}}. \tag{9}$$

Here $\zeta = \xi^{\kappa}$, $\xi = (1 - Y_V^{\infty})/(1 - Y_V^{0})$, where Y^{∞} - vapor concentration in the surrounding medium, Y_d - vapor concentration at the droplet surface, mixture coefficient $\kappa = D_V \rho_m Y_m / \lambda_m$, Y_m − vapor mass concentration in mixture. Note that equation (9) is transcendental, since the specific heat of evaporation L_V in it is taken at the equilibrium temperature T_e. Thus, in the case of noneqiulibrium evaporation of a single droplet under the considered assumptions, the differential equations (7) and (8) have to be solved, in the case of equilibrium evaporation, the problem reduces to solving equation (7) and the transcendental equation (9).

3 NUMERICAL SIMULATION

Let's consider the application of the proposed procedure for calculating characteristics of the heating and evaporation processes of the discrete phase for the problem of multiphase flow modeling in the combustion chamber of an aircraft engine. The scheme of computational domain is represented in fig. 1. Air flow enters fire tube 1 through axial 2 and radial 3 inlets. Liquid fuel enters the combustion chamber through exit nozzle 4 of atomizer 5. Fig. 1a represents the entire computational domain with additional volume imitating a free space. Boundary conditions with fixed mass flow rates and temperatures of gas and liquid were exposed on surfaces corresponding to inlets 2 and 3, 4, with fixed static pressure in the outlet section corresponding to the base of the cylinder imitating a free space. For solid impermeable surfaces, no-slip, adiabatic conditions for continuous medium and elastic reflection conditions for discrete phase were set. The boundary conditions for turbulent characteristics were similar, with a number of simplifications used in [23]. All simulations were performed using FORTRAN program modules on structured curvilinear grid.
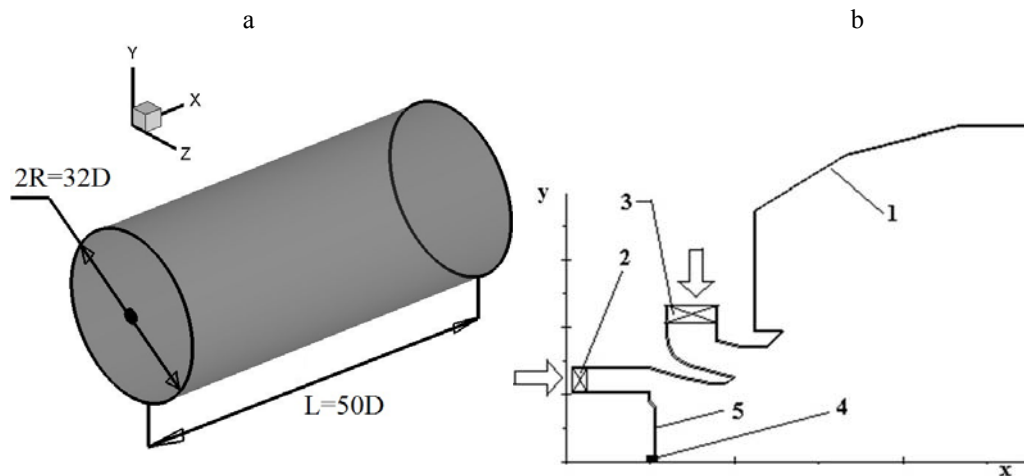
Fig. 1. Computational domain scheme (a) and zoomed view of volume near the inlet section (b), D - exit diameter of the nozzle, D=44.5 mm

3.1 Characteristics of bulk phase

As a first step in the solution of the problem of heating and evaporation of the discrete phase, a numerical solution of the unsteady Navier-Stokes equations in the considered computational domain without discrete phase was obtained. For this step no-slip boundary conditions were set on the surface corresponding to inlet 5 (fig. 1). In the second step, an isothermal problem with a discrete phase was considered, the temperatures of discrete and bulk phases were the same T=298 K. It was assumed that the break up of the fuel film occurs in the immediate vicinity of the nozzle outlet section (inlet 5 fig. 1). It was assumed also that the secondary break up of droplets is determined by the Weber criterion [24], and their coalescence is described by the probability laws of droplets collision. The physical time step for bulk and discrete phases are the same and equals to Δt=10^{-5} s. At this step the influence of injected mass of the discrete phase on the flow structure in primary volume of combustion chamber was estimated. The calculations are performed for the liquid phase - a conventional one-component liquid fuel with chemical formula $C_{12}H_{23}$ at various mass flow rates G_f = 0, 3.75, 5 and 7.5 g/s. In fig. 2 as an example of simulation of the velocity field for an isothermal problem, the fields of the instantaneous longitudinal and circumferential velocity components for fuel mass flow rate G_f= 5 g/s at a time moment corresponding to statistically steady flow t=0.05 s (N_{steps}=5000) are shown. It can be seen from the figure that reverse flow zone (RFZ) exists in the near-axis area of the combustion chamber and velocity magnitude in the entire computational domain does not exceed 80 m/s. Reverse flow zone is used in most modern aviation combustion chambers to stabilize the combustion process, moreover experimental and numerical studies [23] show, that characteristics of RFZ in most cases determine the overall performance of combustion chamber. Thus, it is important for practical reasons to investigate influence of injected discrete phase on geometry of the RFZ.
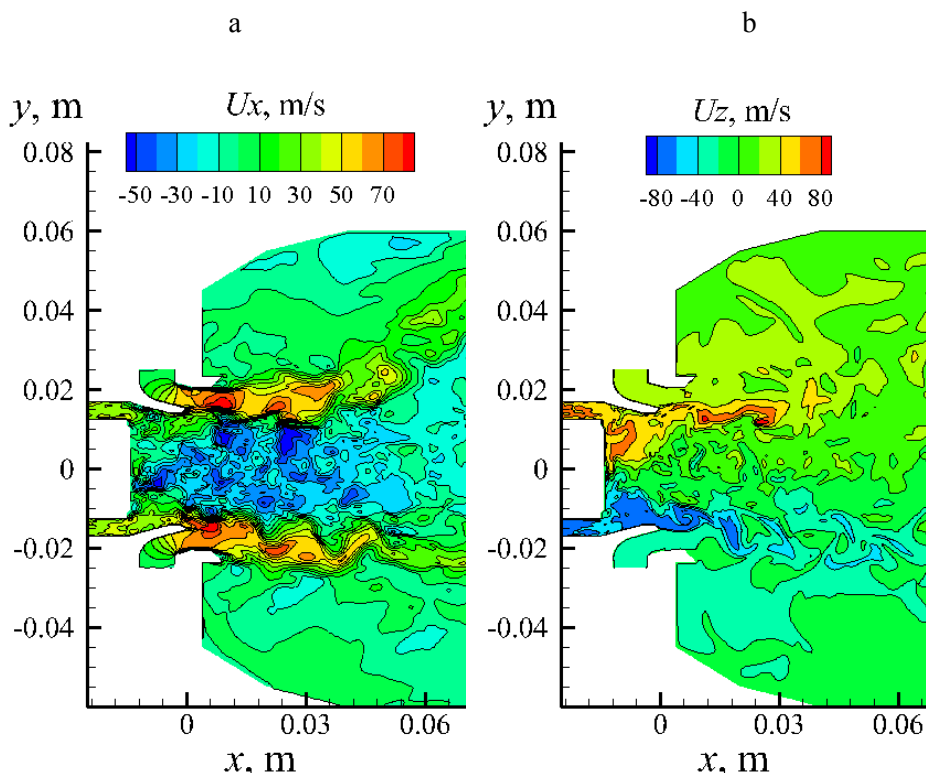
Fig. 2. Instantaneous fields of axial *Ux* (a) and circumferential *Uz* (b) components of the velocity in the middle axial section of the computational domain, isothermal problem, *t*=0.05 s. Colors correspond to the velocity components values

The average geometric characteristics of the RFZ for different mass flow rates of the discrete phase represent in Table 1. Here the spatial characteristic scale is R_0 = 20 mm and abscissa of a section corresponding to maximum width of RFZ are given in last column of the table. Thus, numerical simulations show that the length of the region with large negative values of axial velocity inside the RFZ decreases with increasing of discrete phase mass flow rate G_f.

G_f, g/s	L_{RFZ}/R_0	R_{RFZ}/R_0	X_{RFZ}, mm
0	5.50	0.57	60.0
2.75	6.0	0.95	73.3
5.0	5.49	0.95	84.4
7.5	7.77	0.85	71.2

Table 1. Average geometric sizes of RFZ for different mass flow rates of discrete phase

3.2 Non-isothermal problem with discrete phase

Estimations for low temperatures of the bulk phase and kerosene droplets ($C_p \approx 10^3$ J/K, $L_V \approx 5 \cdot 10^5$ J/kg) show, in particular, that at gas flow temperatures of the order 600 K and initial droplet temperatures of the order 300 K, $\Delta T \approx 300$ K and $x = C_p \Delta T / L_V \approx 0.6$. In this case, the equilibrium approach can lead to a significant error in determining the mass of vaporized

liquid for the droplet and the temperature of its surface. At high temperatures $T > 1000$ K, the heat that evaporates the droplets can be neglected, and the calculation procedure is substantially simplified.

Below results of numerical simulation of non-isothermal flow with discrete phase in computational domain from fig. 1 are represented. Fig. 3 shows mean distributions (averaged for 200 time steps without weight function) of the specific mass concentrations of the liquid phase C_d for pressure level in computational domain $P_c = 5$ atm and gas inlet temperature $T_c = 400$ K. Boundary conditions on surface 4 (fig. 1) for injected droplet temperature is $T_d = 300$ K. Fig. 3-a corresponds to the calculation of droplet evaporation with equilibrium model (without taking into account the influence of fuel vapor concentrations on evaporation rate), fig. 3-b corresponds to proposed non-equilibrium model.
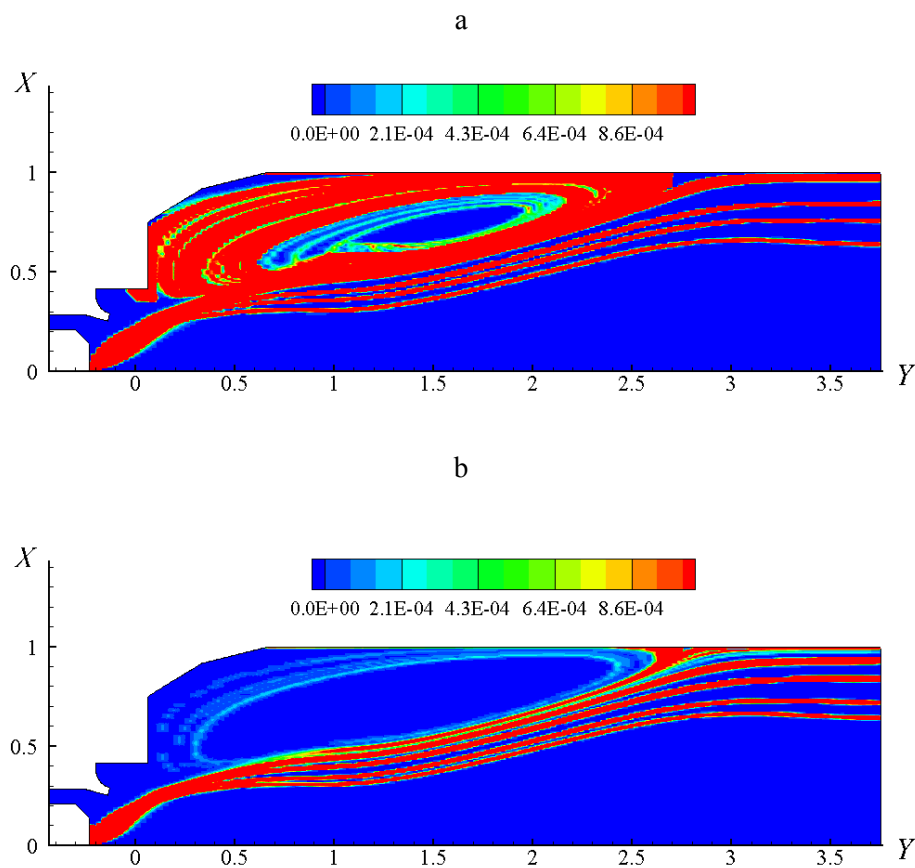
a

b

Fig. 3. Fields of average specific concentration of liquid phase C_d in the middle axial section of computational domain for equilibrium model (a) and non-equilibrium model (b), bulk phase temperatures at the inlet section $T_c = 400$ K, axis corresponds to dimensionless coordinates $X = x/R_0, Y = y/R_0$. Colors correspond to the concentration C_d values

It can be seen from these figures that under considered conditions the distributions of discrete phase obtained with non-equilibrium model, which takes into account influence of saturated vapor pressure on droplet evaporation rate, qualitatively differ from those obtained with equilibrium model. Similar results also occurs at pressure levels in computational domain $P_c = 1–15$ atm. With increasing temperature in the combustion chamber, the effect of

the evaporation non-equilibrium are becoming less visible, and at $T_c = 500$ K there are only quantitative differences in the distributions of the droplet concentrations, even closer these distributions at $T_c = 600$ K and at higher temperatures. The last observation is illustrated in fig. 4 for pressure levels in computational domain $P_c = 5$ atm. Fig. 4-a and 4-b correspond to the calculations with the equilibrium and non-equilibrium models respectively for inlet bulk phase temperature $T_c = 500$ K.
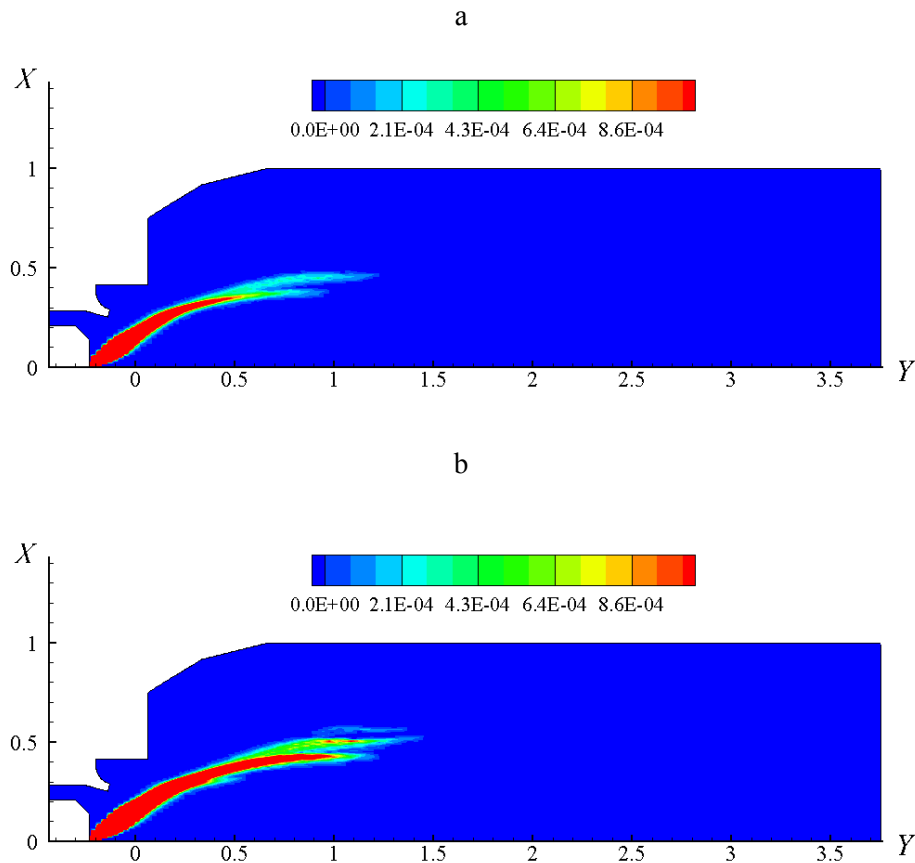
a

b

Fig. 4. Fields of average specific concentration of liquid phase C_d in the middle axial section of computational domain for equilibrium model (a) and non-equilibrium model (b), bulk phase temperatures at the inlet section $T_c = 500$ K, axis corresponds to dimensionless coordinates $X=x/R_0, Y= y/R_0$. Colors correspond to the concentration C_d values

4   CONCLUSION

Results of liquid fuel mixing and evaporation processes numerical simulation in gas-turbine engine combustion chamber are presented. Due to wide variation of thermodynamic parameters in industrial combustors at low temperatures of bulk and discrete phases non-equilibrium evaporation effects could be significant. Multicomponent turbulent flow with discrete phase numerical simulation technique is considered. Model of non-equilibrium evaporation of liquid fuel is proposed, it takes into account in integral form dependence of single droplet evaporation rate on vapor partial pressure near droplet surface. Numerical simulation of isothermal flow with a discrete phase revealed, that interphase exchange of

momentum simulated by source terms in Navier-Stokes equations (at typical mass flow rate ratio G_f/G_{air}<10%) could considerably change the structure of mean flow in computational domain. At mass flow rate ratio G_f/G_{air} =5.5% momentum source, generated by discrete phase leads to increase of mean integral flow scale (mean length of RFZ) on 9% in comparison with single-phase flow. Numerical simulation of non-isothermal flow with a discrete phase revealed that at initial temperatures $T_{d,0}$=300 K and $T_{c,0}$=400 K difference between equilibrium and non-equilibrium models for values of local liquid phase specific concentration can be as large as local mean concentration. Increasing of gas phase temperature to $T_{c,0}$=500 K with fixed $T_{d,0}$ value leads to considerably lower difference between equilibrium and non-equilibrium models results. Thus, increasing of the heat flux per droplet leads to vapor partial pressure increasing near the droplet surface and vapor saturation. Equilibrium droplet evaporation model has lower computational cost, therefore application of this model at moderate and high temperatures of bulk phase T>600..700 K could lead to economy of computational resources while liquid phase evaporation process description accuracy remains the same. I.e. difference connected with non-equilibrium of evaporation process at temperatures T>600..700 K is negligible in described statement.

REFERENCES

[1]   N.A. Fuchs, *Evaporation and droplet growth in gaseous media*, Pergamon Press (1959).

[2]   R.W. Schrage, *A theoretical study of interphase mass transfer*, Columbia University Press (1954).

[3]   D.B. Spalding, *Convective mass transfer. An introduction*, Edward Arnold (1963).

[4]   B.V. Raushenbach, S.A. Belyi, I.V. Bespalov, V.Ya. Borodachev, M.S. Volynskii, A.G. Prudnikov, *Fizicheskiye osnovy rabochego protsessa v kamerakh sgoraniya vozdushno-reaktivnykh dvigateley*, Mashinostroyeniye (1964).

[5]   V.A. Borodin, Yu.F. Dityakin, L.A. Klyachko, V.I. Yagodkin, *Raspylivaniye zhidkostey*, Mashinostroyeniye (1967).

[6]   G.M. Faeth, "Current status of droplet and liquid combustion", *Prog. Energy Combust. Sci*, **3**, 191-224 (1997).

[7]   W.A. Sirignamo, "Fuel droplet vaporization and spray combustion theory", *Prog. Energy Combust. Sci*, **9**, 291-322 (1983).

[8]   A.H. Lefebvre, *Atomization and sprays*, Taylor & Francis (1988).

[9]   S.S. Sazhin, *Droplets and sprays*, Springer (2014).

[10]   S.S. Sazhin, "Advanced models of fuel droplet heating and evaporation", *Prog. Energy Combust. Sci*, **32**, 162-214 (2006).

[11]   C. Yin, "Modeling of heating and evaporation of n-heptane droplets: towards a generic model for fuel droplet/particle conversion", *Fuel*, **141**, 64-73 (2015).

[12]   E. Mahiques, S. Dederichs, C. Beck, P. Kaufmann, J. Kok, "Coupling multicomponent droplet evaporation and tabulated chemistry combustion models for large-eddy simulations", *Int. J. Heat Mass Transfer*, **104**, 51–70 (2017).

[13]   A. Haider, O. Levenspiel, "Drag Coefficient and Terminal Velocity of Spherical and Nonspherical Particles", *J. Powder Technology*, **58**, 63–70 (1989).

[14]   H. Kim, N. Sung, "The effect of ambient pressure on the evaporation of a single droplet and a spray", *Combust. Flame*, **135**, 135-261 (2003).

[15]   W.A. Sirignano, *Fluid dynamics and transport of droplets and sprays*, Cambridge University Press (2010).

[16]   N.E. Kochin, I.A. Kibel, N.V. Roze, *Teoreticheskaya gidrodinamika*, Fizmatgiz, Vol.I., (1963).

[17]   P.D. Hirs, G.M. Pound, *Ispareniye i kondensatsiya*, Metallurgiya, (1966).

[18]   P.R. Spalart, S. Deck, S. Shur, K. Squires, M. Strelets, A. Travin, "A new version of detached-eddy simulation, resistant to ambiguous grid densities", *Theor. Comp. Fluid Dyn.*, **20**, 181-195 (2006).

[19]   J.P. Doormaal, G.D. Raithby, "Enhancements of the simple method for predicting incompressible fluid flows", *Numer. Heat Transfer*, **7** (2), 147-163 (1984).

[20]   V.V. Tretyakov, "Raschet raspredeleniy topliva vo frontovom ustroystve kamery sgoraniya s trekhyarusnym zavikhritelem", *Aviatsionnaya tekhnika*, **4**, 34-38 (2007).

[21]   A.G. Prudnikov, M.S. Volynskii, V.N. Sagalovich, *Protsessy smeseobrazovaniya i goreniya v vozdushno-reaktivnykh dvigatelyakh*, Mashinostroyeniye, (1971).

[22]   J.S. Chin, A.H. Lefebvre, "Steady-state evaporation characteristics of hydrocarbon fuel drops", *AIAA Journal*, **21** (10), 1437-1443 (1983).

[23]   D.L. Zakharov, S.Yu. Krasheninnikov, A.K. Mironov, D.E. Pudovikov, P.D. Toktaliev, "Investigation of unsteady processes, flow properties, and tonal acoustic radiation of a swirling jet", *Fluid Dyn.*, **49** (1), 51-62 (2015).

[24]   A. Frohn, N. Roth, *Dynamics of Droplets*, Springer Verlag, (2000).